Inhomogeneous Knight shift in vortex cores of superconducting FeSe

I. Vinograd, S. P. Edwards, Z. Wang, T. Kissikov, J. K. Byland, J. R. Badger, V. Taufour, and N. J. Curro

Phys. Rev. B **104**, 014502 — Published 7 July 2021

DOI: 10.1103/PhysRevB.104.014502

Inhomogeneous Knight shift in vortex cores of superconducting FeSe

I. Vinograd,[1] S. P. Edwards,[1] Z. Wang,[1] T. Kissikov,[1] J. K. Byland,[1] J. R. Badger,[2] V. Taufour,[1] and N. J. Curro[1]

[1] *Department of Physics and Astronomy, University of California, Davis, California 95616, USA*
[2] *Department of Chemistry, University of California, Davis, California 95616, USA*

(Dated: June 21, 2021)

We report ^{77}Se NMR data in the normal and superconducting states of a single crystal of FeSe for several different field orientations. The Knight shift is suppressed in the superconducting state for in-plane fields, but does not vanish at zero temperature. For fields oriented out of the plane, little or no reduction is observed below T_c. These results reflect spin-singlet pairing emerging from a nematic state with large orbital susceptibility and spin-orbit coupling. The spectra and spin-relaxation rate data reveal electronic inhomogeneity that is enhanced in the superconducting state, possibly arising from enhanced density of states in the vortex cores. Despite the spin polarization of these states, there is no evidence for antiferromagnetic fluctuations.

The iron-based superconductors have attracted broad interest recently because they can host Majorana modes on the surface, at domain walls, and within vortex cores [1–4]. Fe(Se,Te), and Li(Fe,Co)As contain bands with p_z and d_{xz}/d_{yz} character with non-trivial topologies, that give rise to both topological surface states as well as a bulk Dirac point near the Γ point in k-space [5]. FeSe, although topologically trivial, is a particularly interesting case because the superconducting state emerges from a nematic phase that develops below $T_{nem} = 91$K [6]. Moreover, the Fermi energy, E_F, in this system is usually small, such that this system lies close to the BCS-BEC crossover regime [7, 8]. Evidence has emerged that suggests FeSe exhibits a Fulde-Ferell-Larkin-Ovchinnikov (FFLO) phase at high magnetic fields [9]. Thus, a detailed understanding of the nature of the vortices in FeSe is important in the context of a possible FFLO state, but also because its comparison with the topological sister compound Fe(Se,Te) could help to identify new phenomena such as dispersive Majorana modes.

To probe vortex matter it is important to understand both the underlying superconducting state and the spatial inhomogeneity induced by the vortices. The spatial part of the superconducting wavefunction in FeSe appears to have deep minima or nodes [10–14], although direct evidence for spin singlet pairing has been elusive. In the mixed phase, competing orders may give rise to a different electronic structure and spin fluctuations inside the vortex cores, as has been observed in the high temperature superconducting cuprates [15–17] and iron pnictides [18], however little is known about the spin susceptibility in the mixed phase of FeSe.

Information about both the spin component of the wavefunction and the excitations in the vortex cores can be gleaned from nuclear magnetic resonance (NMR) Knight shift and spin lattice relaxation rate measurements. The spin susceptibility of a condensate with singlet pairing vanishes, whereas that with triplet pairing can remain unchanged through T_c. Conventional magnetometry cannot discern these changes because the spin component is much smaller than the orbital component,

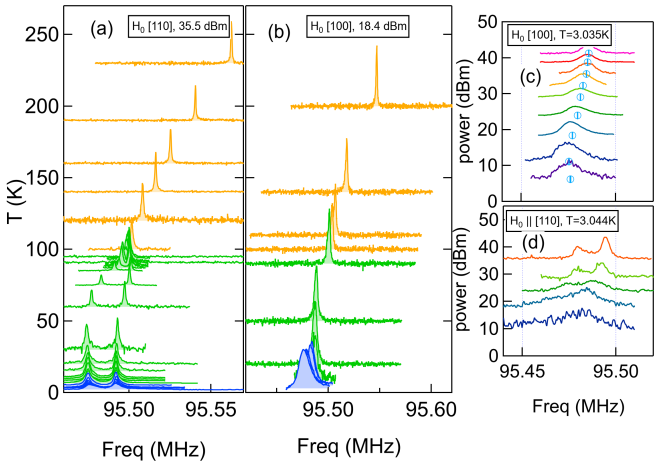

FIG. 1. (a) ^{77}Se NMR spectra (normalized) as a function of temperature for $\mathbf{H}_0 \parallel [110]$ (in tetragonal unit cell) at high rf power (35.5 dBm). Below $T_{nem} = 91$K, the single resonance splits into two separate peaks, corresponding to domains with $\mathbf{H}_0 \parallel \mathbf{a}$ (upper peak) and $\mathbf{H}_0 \parallel \mathbf{b}$ (lower peak) in the nematic phase. (b) Spectra as a function of temperature for $\mathbf{H}_0 \parallel [110]$ at low rf power (18.4 dBm). (c,d) Spectra in the superconducting state as a function of radiofrequency pulse power for $\mathbf{H}_0 \parallel [100]$ and $\mathbf{H}_0 \parallel [110]$, respectively. Blue circles in (c) indicate the first moment of the spectrum. A complete list of temperatures, and spectra for $H_0||[110]$ at low rf power, are available in the supplemental materials [19].

however the Knight shift is usually dominated by the former and is thus one of the only experimental probes of the spin susceptibility of the condensate [7, 8]. To date, Knight shift measurements in the superconducting state have been inconclusive, revealing little or no change below T_c [20–23]. A recent study reported no change in the Knight shift along the c axis in fields up to 16 T, which have been interpreted as evidence for highly spin-polarized Fermi liquid in the BCS-BEC regime [24]. A lack of suppression of the Knight shift may be evidence for spin-triplet pairing [25], but may also reflect thermal instability of the sample due to eddy-current heating

from radiofrequency pulses [26]. In fact, spin-orbit coupling can give rise naturally to a spin-triplet component [27, 28]. To fully characterize the symmetry of the condensate, therefore, it is important to understand the full tensor nature of the Knight shift in the superconducting state.

Here we report ^{77}Se NMR on a high quality single crystal as a function of temperature and field. We find that between 3.6 and 11.7 T, the planar Knight shift is reduced by $\sim 4\%$ from the normal state value below T_c, whereas the out-of-plane component shows no change within the experimental resolution. These results are consistent with spin singlet pairing in the presence of large orbital susceptibility and spin-orbit coupling. Surprisingly, the NMR linewidths broaden inhomogenously by more than a factor of two below T_c for planar fields, but not for $\mathbf{H}_0 \parallel \mathbf{c}$. Accompanying this broadening is a frequency-dependent spin-lattice relaxation rate, T_1^{-1}, that reveals electronic inhomogeneity in the superconducting state. This inhomogeneity cannot be explained by the presence of a conventional vortex lattice, but may reflect an enhanced local density of states within the vortex cores.

Single crystals of FeSe were grown by vapor transport with a tilted two-temperature zone tube furnace [29]. Several samples were characterized with magnetic susceptibility and resistivity measurements, with the best samples having $T_c = 8.9$ K, and RRR defined as the resistance ratio between 250 and 10 K around 19, similar to reported high-quality samples [29]. A large crystal of dimensions $2.4 \times 1.4 \times 0.2$ mm^3 was selected and mounted in a custom-built NMR probe equipped with a dual-axis goniometer. The majority of the experiments were conducted within a variable-temperature cryostat in a high-homogeneity NMR magnet with a field of $H_0 = 11.7294$ T, and some experiments at lower fields were conducted in a PPMS system. In this field, T_c is suppressed to ~ 5.3 K (measured by resistivity) [30]. Spectra (Fig. 1) were collected for field aligned along the tetragonal [110], [100] and [001] directions. The [110] ([1$\bar{1}$0]) direction corresponds to the Fe-Fe bond, and is the **a** (**b**) direction in the nematic phase [31]. The spectra were measured at several temperatures down to 2.1 K using low-power rf pulses ($\pi/2$ pulse widths up to 80μs), sweeping frequency and summing the Fourier transforms. Our results are consistent with previous reports [20–23, 32], and reveal a splitting of the single ^{77}Se resonance below $T_{nem} = 91$ K due to twinning. The resonance frequencies are given by $f = \gamma H_0(1 + K)$, where $\gamma = 8.118$ MHz/T is the gyromagnetic ratio and K is the Knight shift. We fit each resonance to a Gaussian function, and Figs. 2(a,b) shows the temperature dependence of K and the full-width half-maxima, FWHM, for several different field directions. Below T_c, the spectra exhibited a strong dependence on the pulse power, as illustrated in Fig. 1(c,d). The radiofrequency pulses induce eddy currents around the sample, which can lead to Joule heating. As a result, the temperature may temporarily exceed T_c immediately after the pulse. Similar effects have been observed in other superconductors, leading to misinterpretations about the temperature dependence of the Knight shift [26]. As seen in Fig. 1(a), the blue spectra below T_c, measured at high power, reveal little to no shift. The shifts reported in Fig. 2(b) were measured at 18.4 dBm, where there was no power-dependence to the spectra.

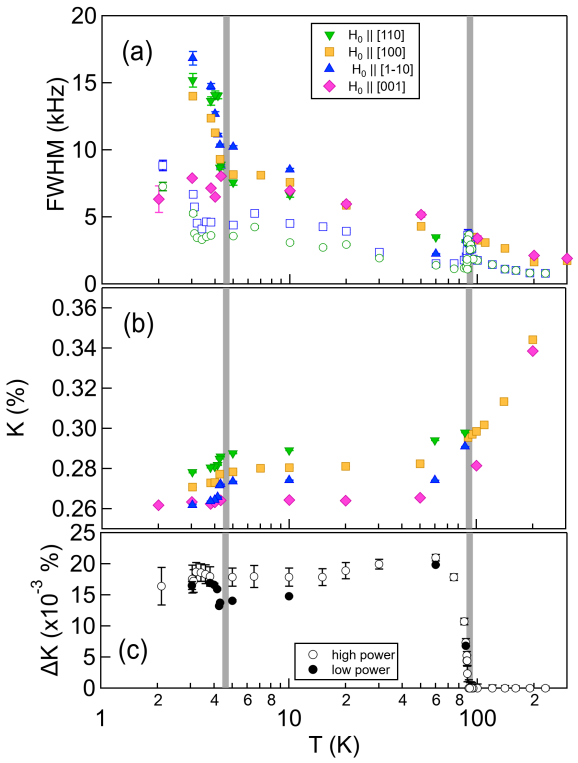

FIG. 2. Linewidth (a) and Knight shifts (b) of the spectra in Fig. 1 as a function of temperature for the field along [110] $\sim$ **a** (▼, ○), [1$\bar{1}$0] $\sim$ **b** (▲, □), [100] (■), and [001] $\sim$ **c** (♦). (c) The in-plane anisotropy $\Delta K = K_a - K_b$ as a function of temperature. Solid (open) points were acquired at low (high) rf power, respectively, as discussed in the text.

The Knight shift arises from the hyperfine interaction between the nuclear spin and the spin and orbital degrees of freedom of the electrons: $\mathcal{H}_{hf} = \mathbf{I} \cdot \mathbb{A}_S \cdot \mathbf{S} + \mathbf{I} \cdot \mathbb{A}_L \cdot \mathbf{L}$, where $\mathbb{A}_{S,L}$ are the hyperfine coupling tensors, and $\mathbf{S}$ and $\mathbf{L}$ are the spin and orbital angular momenta. The Knight shift is given by $K_\alpha = A^L_{\alpha\alpha}\chi^{orb}_{\alpha\alpha} + A^S_{\alpha\alpha}\chi^{spin}_{\alpha\alpha} + (A^S_{\alpha\alpha} + A^L_{\alpha\alpha})\chi^{mixed}_{\alpha\alpha}$, where $\chi^{spin}_{\alpha\alpha}$, $\chi^{orb}_{\alpha\alpha}$, and $\chi^{mixed}_{\alpha\alpha}$ are the static spin, orbital, and mixed susceptibilities at zero wavevector [31, 33]. In the absence of spin-orbit coupling, the mixed term vanishes and the Knight shift is usually decomposed as $K_\alpha = K_{\alpha 0} + A^S_{\alpha\alpha}\chi^{spin}_{\alpha\alpha}$. $K_{\alpha 0}$ is often considered to be a temperature-independent shift

arising from a Van-Vleck orbital susceptibility, however, this decomposition breaks down in the presence of spin-orbit coupling [34]. Moreover, theoretical calculations have revealed that $\chi^{orb}_{\alpha\alpha} \gg \chi^{spin}_{\alpha\alpha}, \chi^{mixed}_{\alpha\alpha}$ due to the multiorbital nature of the band structure and nematic instability [31]. As a result, the relationship between K_α and the bulk susceptibility, $\chi = \chi^{spin} + \chi^{orb} + 2\chi^{mixed}$, is complicated. Nevertheless, we find that K_α varies linearly with χ above T_{nem}, as shown in the inset of Fig. 3. Linear fits to the data yield parameters close to previously reported values [23].

For spin-singlet pairing, χ^{spin} and χ^{mixed} should vanish in the superconducting state, giving rise to a suppression of K below T_c, as observed in Fig. 3. For planar fields, $K_{a,b}$ is suppressed by about 100 ± 15 ppm in both domains, as well as for the [100] direction oriented 45° to the Fe-Fe bond direction. This magnitude of suppression does not change significantly at lower fields. For out of plane fields, any change in K_c is within the noise, but is less than ~ 10 ppm. These results are also independent of applied field, and seem to be consistent with previous reports [24, 35], however more careful studies at lower fields along [001] should be conducted to check for heating effects. For fields other than 11.7T pulse powers of about 22dB have been used that exceed the threshold for heating. By comparison with the power dependence of the low temperature data measured at 11.7T we estimate lower error bars that indicate that the Knight shift decrease could be nearly twice the magnitude measured with pulses smaller than 22dB.

Note that $K_\alpha(T \to 0) \neq K_{\alpha 0}$, or in other words the low temperature limit of the shift does not equal the intercepts from the $K - \chi$ plot. In fact, χ^{orb} is strongly temperature dependent, so $K_{\alpha 0}$ does not represent a temperature independent Van-Vleck term. The low temperature shift reflects a finite χ^{orb}, since the spin component vanishes for singlet pairing; however impurity states may play a role [36]. Determining how much χ^{spin}, χ^{orb} and χ^{mixed} are suppressed below T_c will likely require detailed theoretical calculations [31]. It is noteworthy that the difference $K_a - K_b$, shown in Fig. 2(c), exhibits a subtle enhancement below T_c. This observation suggests that the superconductivity is slightly anisotropic in the two domains, and may reflect an anisotropy in the coherence lengths, $\xi_{a,b}$.

Below T_c the spectra for both domains broaden and become asymmetric with a high frequency tail, as observed in Fig. 1(c,d) and 2(a). At 230 K the FWHM of the spectrum is ~ 0.08 kHz, and fits with a Voigt profile give a Gaussian contribution to the linewidth (~ 0.04 kHz) that is close to the second moment of the nuclear spin dipole moments of the lattice (~ 0.06 kHz). The excess inhomogeneous broadening above T_c may be due to either macroscopic or microscopic strain fields [37]. The crystals were initially secured to the goniometer with a light coat of superglue and the coil fit loosely around the sample. In this case, the observed linewidths were smaller (open points in Fig. 2(a)), reflecting the high quality of this crystal. In later measurements, the crystal was remounted and we observed the linewidth increase by a factor ~ 2 (solid points in Fig. 2(a)). It is possible that remounting the crystal introduced inhomogeneous macroscopic strain fields. Non-magnetic impurities such as Fe vacancies are known to exist in the lattice [11], which may also be a source of local strain and inhomogeneous broadening in the normal state.

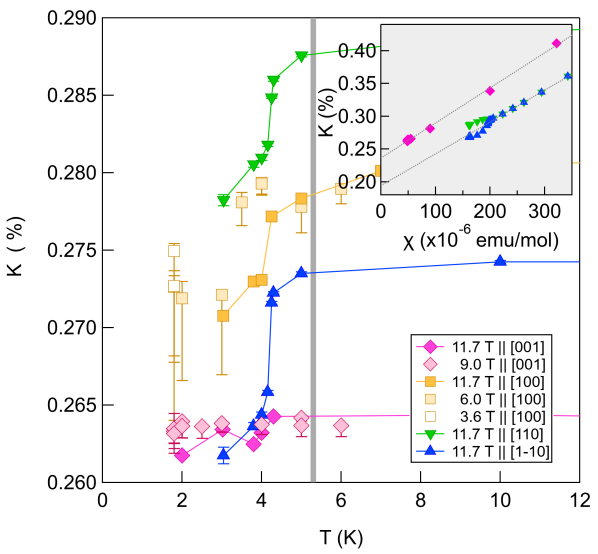

FIG. 3. K_α versus temperature for fields and orientations. (INSET) K versus χ for in the normal state, using susceptibility data from [23]. The dotted lines indicate the best linear fits, with parameters $K_{0a} = 0.194 \pm 0.002\%$, $A_{aa} = 27.1 \pm 0.3$ kOe/μ_B, $K_{0c} = 0.236 \pm 0.001\%$, and $A_{cc} = 29.9 \pm 0.5$ kOe/μ_B, as described in the text.

Regardless of the linewidth in the normal state, an even larger increase of linewidth is observed below T_c, which is unexpected. A vortex lattice certainly gives rise to a distribution of local magnetic fields, $B(\mathbf{r})$, and in very low fields $B \ll B_{c2}$, the second moment of the field distribution can be estimated as $\Delta B^2 \approx 0.00371 \phi_0^2 \lambda^{-4}$, where ϕ_0 is the flux quantum, and the penetration depths are $\lambda_a = 446$ nm, $\lambda_c = 1320$ nm [38, 39]. There are important corrections to this expression in the higher fields where our measurements were conducted [40], however after accounting for these we estimate that the normal state spectra should broaden by only ~ 8 Hz, three orders of magnitude smaller than the enhancement observed in Fig. 2(a) [19].

Since the field distribution alone is unable to capture the asymmetric broadening, we hypothesize the presence of a spatially-varying Knight shift, $K_\alpha(\mathbf{r})$, that is equal to the normal state value within the vortex cores and decays to $K_\alpha(T \to 0)$ outside. The spectrum is

given by the histogram of the local resonance frequency, $f(\mathbf{r}) = \gamma B(\mathbf{r})(1 + K_\alpha(\mathbf{r}))$. The exact shape of the spectrum depends on microscopic details, but if the spatial variation δK is equal to the 100 ppm suppression observed in Fig. 3, the spectrum will broaden by ~ 10 kHz, which agrees well with the excess linewidth below T_c in Fig. 2(a). These results suggest that the local spin susceptibility within the vortex cores is identical to that in the normal state.

This interpretation is supported by T_1^{-1} measurements. Fig. 4(a) shows $(T_1T)^{-1}$ versus temperature. The data in the normal state agree well with published results [20, 23, 41]. This quantity drops due to the superconductivity, and becomes inhomogeneous in the mixed phase. Fig. 4(b) shows that T_1^{-1} increases by nearly a factor of two in the high frequency tails of the spectra in the superconducting state, which correspond with the vortex cores. Localized Caroli-deGennes-Matricon (CdGM) electronic states normally exist within isolated cores [42]. At higher fields quasiparticles from different cores can propagate coherently across multiple vortices, and the energy spectrum becomes dispersive, with gapless excitations remaining within the vortex cores that give rise to a finite local density of states (LDOS) which should be manifest in any technique sensitive to low energy excitations [43–46]. Indeed enhanced T_1^{-1} has been identified within the vortex cores of both conventional [47] and unconventional superconductors [15, 48].

There are, however, important differences between FeSe and previous observations on other superconductors. In the cuprates, the excess relaxation rate has been attributed to antiferromagnetic fluctuations from a competing ground state to superconductivity [15, 48], as well as from Doppler-shifted quasiparticles associated with d-wave nodes [49]. In such cases $(T_1T)^{-1}$ exhibits a strong Curie-Weiss divergence within the cores, whereas outside the cores $(T_1T)^{-1}$ remains temperature independent. In the s-wave superconductor $LaRu_4P_{12}$, $(T_1T)^{-1}$ in the cores is also strongly temperature dependent, and even exceeds the value in the normal state [47]. In the case of FeSe, $(T_1T)^{-1}$ exhibits Curie-Weiss behavior in the normal state (dotted lines in Fig. 4a), but drops below T_c. This behavior has been attributed to antiferromagnetic spin fluctuations that are gapped by the superconductivity [50, 51]. The open circles (squares) in Fig. 4(a,c) show the temperature dependence at the upper end of the spectra in the superconducting state. $(T_1T)^{-1}$ in the vortex cores changes only by a factor of two from the background rate, remaining well below the normal state value, and exhibits the same trend with temperature as the background. These results suggest the absence of any spin fluctuations within the normal cores of FeSe.

FeSe appears unique in that there is a $\mathbf{q} = 0$ spin response in the vortex cores. It is unclear whether this behavior could be related to either a proximity to the BCS-BEC crossover, or either a Fulde-Ferrell-Larkin-Ovchinnikov (FFLO) phase [8, 9] or a field-induced spin density wave [52] for parallel fields above $H^* = 24$ T. A true FFLO phase should exhibit both segmented vortex lines and normal planes where the LDOS reaches the normal state values, giving rise to inhomogeneously broadened NMR spectra. Although $H_0 \sim 0.5H^*$ in our experiments, the inhomogeneity we observe already indicates the presence of large spin polarization in spatial regions where the superconducting order vanishes. It is noteworthy that the $\mathbf{q} = 0$ susceptibility in FeSe is dominated by orbital contributions, whereas the finite $\mathbf{q}$ response is dominated by spin fluctuations [31]. Condensation of singlet pairs enables us to probe the small spin response at $\mathbf{q} = 0$. In $Ba(Fe,Co)_2As_2$, finite $\mathbf{q}$ spin fluctuations can freeze and exhibit long range antiferromagnetism in vortex cores [18]. In FeSe we see no evidence for such behavior, which may be due to the presence of nematic

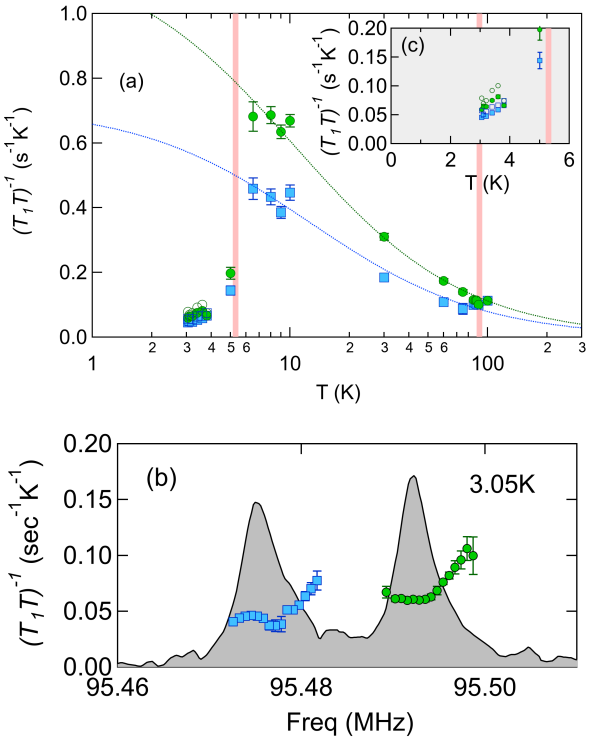

FIG. 4. (a) $(T_1T)^{-1}$ versus temperature (symbols defined in Fig. 2) for $\mathbf{H}_0 \parallel [110]$ at 11.7 T. The dotted lines are best fits to a Curie-Weiss form, as described in the text. (b) $(T_1T)^{-1}$ versus frequency at 3.05K in the mixed phase, revealing an enhanced rate within the vortex cores. The spectrum is shown in gray. T_1^{-1} and spectra were acquired with high power rf pulses. T_1 was measured by integrating the intensity over small windows of 0.7kHz separately and fit with a stretched relaxation curve for spin 1/2. The stretching exponent is 0.85±0.05 and shows no frequency dependence. Heating reduces the linewidth, so we observe a frequency dependent relaxation rate over a smaller frequency range. Measurements at low power are provided in [19].

order and the different contribution of orbital versus spin susceptibility. The absence of such fluctuations suggests that the high field phase is unrelated to SDW order, at least for in-plane fields [52, 53]. It may be that the finite spin shift within the cores arises due to the low energy excitations associated with the deep minima in the gap function.

In summary, we find that the Knight shift is suppressed below T_c for in-plane fields, but see little to no suppression for field along the c-axis. The spectra are inhomogeneously broadened below T_c, and T_1^{-1} becomes frequency-dependent. These observations are consistent with a finite LDOS within the vortex cores. We find no evidence of competing antiferromagnetic fluctuations in the vortex cores. Further studies at higher fields or with Te doping should shed light on the unusual nature of the vortex states in this system.

Acknowledgment. We acknowledge helpful discussions with B. Andersen, E. da Silva Neto, M. Walker, and R. Fernandes, and thank P. Klavins for assistance in the lab. Work at UC Davis was supported by the NSF under Grants No. DMR-1807889, and synthesis of single crystals was supported by the UC Laboratory Fees Research Program ID LFR-20-653926.

[1] E. J. König and P. Coleman, Crystalline-symmetry-protected helical Majorana modes in the iron pnictides, Phys. Rev. Lett. **122**, 207001 (2019).

[2] P. Zhang, Z. Wang, X. Wu, K. Yaji, Y. Ishida, Y. Kohama, G. Dai, Y. Sun, C. Bareille, K. Kuroda, T. Kondo, K. Okazaki, K. Kindo, X. Wang, C. Jin, J. Hu, R. Thomale, K. Sumida, S. Wu, K. Miyamoto, T. Okuda, H. Ding, G. D. Gu, T. Tamegai, T. Kawakami, M. Sato, and S. Shin, Multiple topological states in iron-based superconductors, Nat. Phys. **15**, 41 (2018).

[3] L. Kong, L. Cao, S. Zhu, M. Papaj, G. Dai, G. Li, P. Fan, W. Liu, F. Yang, X. Wang, S. Du, C. Jin, L. Fu, H.-J. Gao, and H. Ding, Tunable vortex Majorana zero modes in LiFeAs superconductor, arXiv e-prints , arXiv:2010.04735 (2020), arXiv:2010.04735 [cond-mat.supr-con].

[4] Z. Wang, J. O. Rodriguez, L. Jiao, S. Howard, M. Graham, G. D. Gu, T. L. Hughes, D. K. Morr, and V. Madhavan, Evidence for dispersing 1d majorana channels in an iron-based superconductor, Science **367**, 104 (2020).

[5] Z. Wang, P. Zhang, G. Xu, L. K. Zeng, H. Miao, X. Xu, T. Qian, H. Weng, P. Richard, A. V. Fedorov, H. Ding, X. Dai, and Z. Fang, Topological nature of the $FeSe_{0.5}Te_{0.5}$ superconductor, Phys. Rev. B **92**, 115119 (2015).

[6] A. Kreisel, P. J. Hirschfeld, and B. M. Andersen, On the remarkable superconductivity of FeSe and its close cousins, Symmetry **12**, 1402 (2020).

[7] T. Hanaguri, S. Kasahara, J. Bker, I. Eremin, T. Shibauchi, and Y. Matsuda, Quantum vortex core and missing pseudogap in the multiband BCS-BEC crossover superconductor FeSe, Phys. Rev. Lett. **122**, 077001 (2019).

[8] T. Shibauchi, T. Hanaguri, and Y. Matsuda, Exotic superconducting states in FeSe-based materials, J. Phys. Soc. Japan **89**, 102002 (2020).

[9] S. Kasahara, Y. Sato, S. Licciardello, M. Čulo, S. Arsenijević, T. Ottenbros, T. Tominaga, J. Bker, I. Eremin, T. Shibauchi, J. Wosnitza, N. Hussey, and Y. Matsuda, Evidence for an fulde-ferrell-larkin-ovchinnikov state with segmented vortices in the BCS-BEC-crossover superconductor FeSe, Phys. Rev. Lett. **124**, 107001 (2020).

[10] P. Bourgeois-Hope, S. Chi, D. Bonn, R. Liang, W. Hardy, T. Wolf, C. Meingast, N. Doiron-Leyraud, and L. Taillefer, Thermal conductivity of the iron-based superconductor FeSe: Nodeless gap with a strong two-band character, Phys. Rev. Lett. **117**, 097003 (2016).

[11] P. O. Sprau, A. Kostin, A. Kreisel, A. E. Böhmer, V. Taufour, P. C. Canfield, S. Mukherjee, P. J. Hirschfeld, B. M. Andersen, and J. C. S. Davis, Discovery of orbital-selective cooper pairing in FeSe, Science **357**, 75 (2017).

[12] L. Jiao, C.-L. Huang, S. Rßler, C. Koz, U. K. Rßler, U. Schwarz, and S. Wirth, Superconducting gap structure of FeSe, Sci. Rep. **7**, 44024 (2017).

[13] P. K. Biswas, A. Kreisel, Q. Wang, D. T. Adroja, A. D. Hillier, J. Zhao, R. Khasanov, J.-C. Orain, A. Amato, and E. Morenzoni, Evidence of nodal gap structure in the basal plane of the FeSe superconductor, Phys. Rev. B **98**, 180501 (2018).

[14] F. Hardy, M. He, L. Wang, T. Wolf, P. Schweiss, M. Merz, M. Barth, P. Adelmann, R. Eder, A.-A. Haghighirad, and C. Meingast, Calorimetric evidence of nodal gaps in the nematic superconductor FeSe, Phys. Rev. B **99**, 035157 (2019).

[15] V. F. Mitrovic, E. E. Sigmund, M. Eschrig, H. N. Bachman, W. P. Halperin, A. P. Reyes, P. Kuhns, and W. G. Moulton, Spatially resolved electronic structure inside and outside the vortex cores of a high-temperature superconductor, Nature **413**, 6855 (2001).

[16] B. Lake, K. Lefmann, N. B. Christensen, G. Aeppli, D. F. McMorrow, H. M. Ronnow, P. Vorderwisch, P. Smeibidl, N. Mangkorntong, T. Sasagawa, M. Nohara, and T. Takagi, Three-dimensionality of field-induced magnetism in a high-temperature superconductor, Nat. Mater. **4**, 658 (2005).

[17] B. Lake, G. Aeppli, K. N. Clausen, D. F. McMorrow, K. Lefmann, N. E. Hussey, N. Mangkorntong, M. Nohara, H. Takagi, T. E. Mason, and A. Schrder, Spins in the vortices of a high-temperature superconductor, Science **291**, 5509 (2001).

[18] J. Larsen, B. M. Uranga, G. Stieper, S. L. Holm, C. Bernhard, T. Wolf, K. Lefmann, B. M. Andersen, and C. Niedermayer, Competing superconducting and magnetic order parameters and field-induced magnetism in electron-dopedBa(fe1-xCox)2as2, Physical Review B **91**, 024504 (2015).

[19] See Supplemental Material at [URL will be inserted by publisher] for [give brief description of material].

[20] S.-H. Baek, D. V. Efremov, J. M. Ok, J. S. Kim, J. van den Brink, and B. Büchner, Orbital-driven nematicity in FeSe, Nat. Mater. **14**, 210 (2015).

[21] P. Wiecki, M. Nandi, A. E. Bhmer, S. L. Bud'ko, P. C. Canfield, and Y. Furukawa, NMR evidence for static local nematicity and its cooperative interplay with low-energy magnetic fluctuations in FeSe under pressure, Phys. Rev.

B **96**, 180502 (2017).
[22] S.-H. Baek, D. V. Efremov, J. M. Ok, J. S. Kim, J. van den Brink, and B. Bchner, Nematicity and in-plane anisotropy of superconductivity in β-FeSe detected by ^{77}Se nuclear magnetic resonance, Phys. Rev. B **93**, 180502 (2016).
[23] J. Li, B. Lei, D. Zhao, L. Nie, D. Song, L. Zheng, S. Li, B. Kang, X. Luo, T. Wu, and X. Chen, Spin-orbital-intertwined nematic state in FeSe, Phys. Rev. X **10**, 011034 (2020).
[24] S. Molatta, D. Opherden, J. Wosnitza, Z. T. Zhang, T. Wolf, H. v. Löhneysen, R. Sarkar, P. K. Biswas, H. J. Grafe, and H. Kühne, Superconductivity of highly spin-polarized electrons in FeSe probed by ^{77}Se NMR, arXiv e-prints , arXiv:2010.10128 (2020), arXiv:2010.10128 [cond-mat.supr-con].
[25] K. Ishida, H. Mukuda, Y. Kitaoka, K. Asayama, Z. Q. Mao, Y. Mori, and Y. Maeno, Spin-triplet superconductivity in Sr_2RuO_4 identified by ^{17}O Knight shift, Nature **396**, 658 (1998).
[26] A. Pustogow, Y. Luo, A. Chronister, Y.-S. Su, D. A. Sokolov, F. Jerzembeck, A. P. Mackenzie, C. W. Hicks, N. Kikugawa, S. Raghu, E. D. Bauer, and S. E. Brown, Constraints on the superconducting order parameter in Sr_2RuO_4 from oxygen-17 nuclear magnetic resonance, Nature **574**, 72 (2019).
[27] V. Cvetkovic and O. Vafek, Space group symmetry, spin-orbit coupling, and the low-energy effective Hamiltonian for iron-based superconductors, Phys. Rev. B **88**, 134510 (2013).
[28] O. Vafek and A. V. Chubukov, Hund interaction, spin-orbit coupling, and the mechanism of superconductivity in strongly hole-doped iron pnictides, Phys. Rev. Lett. **118**, 087003 (2017).
[29] A. E. Bhmer, V. Taufour, W. E. Straszheim, T. Wolf, and P. C. Canfield, Variation of transition temperatures and residual resistivity ratio in vapor-grown FeSe, Phys. Rev. B **94**, 024526 (2016).
[30] S. I. Vedeneev, B. A. Piot, D. K. Maude, and A. V. Sadakov, Temperature dependence of the upper critical field of FeSe single crystals, Phys. Rev. B **87**, 134512 (2013).
[31] R. Zhou, D. D. Scherer, H. Mayaffre, P. Toulemonde, M. Ma, Y. Li, B. M. Andersen, and M.-H. Julien, Singular magnetic anisotropy in the nematic phase of FeSe, npj Quantum Materials **5**, 93 (2020).
[32] R. X. Cao, J. Hu, J. Dong, J. B. Zhang, X. S. Ye, Y. F. Xu, D. A. Chareev, A. N. Vasiliev, B. Wu, X. H. Zeng, Q. L. Wang, and G. Wu, Observation of orbital ordering and origin of the nematic order in FeSe, New J. Phys. **21**, 103033 (2019).
[33] K. R. Shirer, A. C. Shockley, A. P. Dioguardi, J. Crocker, C. H. Lin, N. apRoberts Warren, D. M. Nisson, P. Klavins, J. C. Cooley, Y.-f. Yang, and N. J. Curro, Long range order and two-fluid behavior in heavy electron materials, Proc. Natl. Acad. Sci. **109**, E3067 (2012).
[34] D. M. Nisson and N. J. Curro, Nuclear magnetic resonance Knight shifts in the presence of strong spin-orbit and crystal-field potentials, New J. Phys. **18**, 073041 (2016).
[35] H. Kotegawa, S. Masaki, Y. Awai, H. Tou, Y. Mizuguchi, and Y. Takano, Evidence for unconventional superconductivity in arsenic-free iron-based superconductor FeSe: A ^{77}Se-NMR study, J. Phys. Soc. Japan **77**, 113703 (2008).
[36] N. Curro, T. Caldwell, E. Bauer, L. Morales, M. Graf, Y. Bang, A. Balatsky, J. Thompson, and J. Sarrao, Unconventional superconductivity in $PuCoGa_5$, Nature **434**, 622 (2005).
[37] S. Tan, Y. Zhang, M. Xia, Z. Ye, F. Chen, X. Xie, R. Peng, D. Xu, Q. Fan, H. Xu, J. Jiang, T. Zhang, X. Lai, T. Xiang, J. Hu, B. Xie, and D. Feng, Interface-induced superconductivity and strain-dependent spin density waves in FeSe/SrTiO3 thin films, Nat. Mater. **12**, 634 (2013).
[38] J. E. Sonier, Muon spin rotation studies of electronic excitations and magnetism in the vortex cores of superconductors, Rep. Progr. Phys. **70**, 1717 (2007).
[39] M. Abdel-Hafiez, J. Ge, A. N. Vasiliev, D. A. Chareev, J. V. de Vondel, V. V. Moshchalkov, and A. V. Silhanek, Temperature dependence of lower critical field $H_{c1}(T)$ shows nodeless superconductivity in FeSe, Phys. Rev. B **88**, 174512 (2013).
[40] A. Maisuradze, R. Khasanov, A. Shengelaya, and H. Keller, Comparison of different methods for analyzing μSR line shapes in the vortex state of type-II superconductors, J. Phys.: Condens. Matter **21**, 075701 (2009).
[41] A. Shi, T. Arai, S. Kitagawa, T. Yamanaka, K. Ishida, A. E. Bhmer, C. Meingast, T. Wolf, M. Hirata, and T. Sasaki, Pseudogap behavior of the nuclear spin–lattice relaxation rate in FeSe probed by ^{77}Se-NMR, J. Phys. Soc. Japan **87**, 013704 (2018).
[42] C. Caroli, P. D. Gennes, and J. Matricon, Bound fermion states on a vortex line in a type II superconductor, Phys. Lett. A **9**, 307 (1964).
[43] S. Dukan and Z. Tešanović, Superconductivity in a high magnetic field: Excitation spectrum and tunneling properties, Phys. Rev. B **49**, 13017 (1994).
[44] M. R. Norman, A. H. MacDonald, and H. Akera, Magnetic oscillations and quasiparticle band structure in the mixed state of type-II superconductors, Phys. Rev. B **51**, 5927 (1995).
[45] M. Ichioka, A. Hasegawa, and K. Machida, Field dependence of the vortex structure ind-wave ands-wave superconductors, Phys. Rev. B **59**, 8902 (1999).
[46] J.-X. Zhu, Local electronic structure in superconductors under a magnetic field, in *Bogoliubov-de Gennes Method and Its Applications* (Springer International Publishing, Cham, 2016) pp. 111–139.
[47] Y. Nakai, Y. Hayashi, K. Kitagawa, K. Ishida, H. Sugawara, D. Kikuchi, and H. Sato, Evidence of the bound states of the vortex state in ans-wave superconductor proved by NMR measurements, J. Phys. Soc. Japan **77**, 333 (2008).
[48] V. F. Mitrović, E. E. Sigmund, W. P. Halperin, A. P. Reyes, P. Kuhns, and W. G. Moulton, Antiferromagnetism in the vortex cores of $YBa_2Cu_3O_{7-\delta}$, Phys. Rev. B **67**, 220503 (2003).
[49] N. Curro, C. Milling, J. Haase, and C. Slichter, Local-field dependence of the O-17 spin-lattice relaxation and echo decay rates in the mixed state of $YBa_2Cu_3O_7$, Phys. Rev. B **62**, 3473 (2000).
[50] T. Imai, K. Ahilan, F. L. Ning, T. M. McQueen, and R. J. Cava, Why does undoped FeSe become a high-Tc superconductor under pressure?, Phys. Rev. Lett. **102**, 177005 (2009).
[51] S. Mukherjee, A. Kreisel, P. Hirschfeld, and B. M. Andersen, Model of electronic structure and superconductivity

in orbitally ordered FeSe, Phys. Rev. Lett. **115**, 026402 (2015).

[52] N. Zhou, Y. Sun, C. Y. Xi, Z. S. Wang, Y. F. Zhang, C. Q. Xu, Y. Q. Pan, J. J. Feng, Y. Meng, X. L. Yi, L. Pi, T. Tamegai, X. Xing, and Z. Shi, Disorder-robust high-field superconducting phase of FeSe single crystals, arXiv e-prints , arXiv:2102.02353 (2021), arXiv:2102.02353 [cond-mat.supr-con].

[53] B. L. Young, R. R. Urbano, N. J. Curro, J. D. Thompson, J. L. Sarrao, A. B. Vorontsov, and M. J. Graf, Microscopic evidence for field-induced magnetism in $CeCoIn_5$, Phys. Rev. Lett. **98**, 036402 (2007).